Acta Cryst. (1994). A**50**, 475–480

Dynamical Diffraction in the Laue Case with Borrmann Absorption

BY T. FUKAMACHI AND R. NEGISHI

Department of Electronic Engineering, Saitama Institute of Technology, 1690 *Fusaiji, Okabe, Ohsato, Saitama* 369-02, *Japan*

AND T. KAWAMURA

Department of Physics, Yamanashi University, Kofu, Yamanashi 400, *Japan*

(*Received* 21 *April* 1993; *accepted* 13 *December* 1993)

Abstract

Dynamical X-ray diffraction is studied on the basis of a theory presented by Fukamachi & Kawamura [*Acta Cryst.* (1993), A**49**, 384–388], which takes account of Borrmann absorption and is applicable even when the real part of that atomic scattering factor is zero. Rocking curves and integrated reflecting powers are calculated in both the symmetric and the asymmetric Laue cases. A nontransparent effect is found in the rocking curves of the transmitted beam. An enhancement of abnormal transmission intensity is found in the asymmetric case. The *Pendellösung* fringes observed in the rocking curves and the integrated reflecting powers are studied and the precision of the crystal structure factors determined from the *Pendellösung* fringes is discussed.

1. Introduction

In studies of X-ray dynamical theory, most workers have paid attention to the case where the real part of the atomic scattering factors is much larger than the imaginary part. By tuning X-ray energy from synchrotron radiation, it becomes possible to measure the dynamical diffraction when the imaginary part of the atomic scattering factor is larger than the real part (Fukamachi *et al.*, 1993). Fukamachi & Kawamura (1993) (hereinafter referred to as FK) have studied dynamical diffraction by revising the conventional dynamical theory. They have discussed diffraction effects for which the real part of the X-ray polarizability is zero. In the Bragg case, the rocking curve shows narrower width than that having no absorption effect [Kato (1992) showed the same results theoretically]. In the Laue case, the rocking curve shows *Pendellösung* fringes induced by the imaginary part of the scattering factor.

This paper, based on the FK theory, studies rocking curves and integrated reflecting powers in the Laue case for various ratios of the real and imaginary parts of the X-ray polarizability.

2. Theoretical basis

The Fourier transform of the X-ray polarizability, χ_h (4π times the polarizability), is expressed by

$$\chi_h = \chi_{hr} + i\chi_{hi}. \tag{1}$$

Here, $\chi_{hr} = |\chi_{hr}| \exp(i\alpha_{hr})$ is the Fourier transform of the real part of the X-ray polarizability and $\chi_{hi} = |\chi_{hi}| \exp(i\alpha_{hi})$ is that of the imaginary part. The phase difference is given by

$$\delta = \alpha_{hi} - \alpha_{hr}. \tag{2}$$

In the following, it is convenient to define $\overline{\chi}_h$ as

$$\overline{\chi}_h^2 = |\chi_{hr}|^2 + |\chi_{hi}|^2. \tag{3}$$

We also define the following parameters:

$$k = |\chi_{hr}|/|\chi_{hi}|, \tag{4}$$

$$b = 2^{1/2}/(k^2+1)^{1/2} = 2^{1/2}|\chi_{hi}|/\overline{\chi}_h, \tag{5}$$

$$p = k/(k^2+1) = |\chi_{hr}||\chi_{hi}|/\overline{\chi}_h^2 \tag{6}$$

and

$$g = g_0/(k^2+1)^{1/2} = \chi_{0i}/\overline{\chi}_h, \tag{7}$$

where $g_0 = \chi_{0i}/|\chi_{hi}|$. The parameters b, p and g are finite even if k becomes infinite (no absorption).

The diffracted and transmitted intensities P_h and P_d in the Laue case are given by

$$P_h/P_0 = \exp(-\mu H')(1 - 2p\sin\delta)\{\sin^2(sH\,\mathrm{Re}\,L^{1/2}) + \sinh^2(sH\,\mathrm{Im}\,L^{1/2})\}/|L^{1/2}|^2 \tag{8}$$

and

$$\begin{aligned} P_d/P_0 = \exp(-\mu H')\{&[(|L^{1/2}|^2 - W^2 - g'^2) \\ &\times \cos(2sH\,\mathrm{Re}\,L^{1/2}) \\ &+ (|L^{1/2}|^2 + W^2 + g'^2)\cosh(2sH\,\mathrm{Im}\,L^{1/2})]/2 \\ &- (g'\,\mathrm{Re}\,L^{1/2} - W\,\mathrm{Im}\,L^{1/2})\sin(2sH\,\mathrm{Re}\,L^{1/2}) \\ &- (W\,\mathrm{Re}\,L^{1/2} + g'\,\mathrm{Im}\,L^{1/2}) \\ &\times \sinh(2sH\,\mathrm{Im}\,L^{1/2})\}/|L^{1/2}|^2. \end{aligned} \tag{9}$$

Here, P_0 is the incident X-ray intensity, H the crystal

ISSN 0108-7673

thickness and μ the mean linear absorption coefficient. The parameter g' is related to g by

$$g' = g \sin\theta \cos\beta/|\cos\theta_1 \cos\theta_2|^{1/2}. \quad (10)$$

In (8) and (9), s and H' are given by

$$s = \pi k_{0r}\overline{\chi}_h/|\cos\theta_1 \cos\theta_2|^{1/2} \quad (11)$$

and

$$H' = H \cos\theta \sin\beta/(\cos\theta_1 \cos\theta_2). \quad (12)$$

The real part of the wave vector in a crystal is k_{0r} and the Bragg angle is θ. The angles θ_1, θ_2 and β are those of the transmitted beam, the diffracted beam and the scattering vector **h**, respectively, with respect to the surface normal directed inwards.

$$\mu H' = -2sHg_0/(k^2+1)^{1/2}. \quad (13)$$

The deviation parameter W gives the measure of difference from the exact Bragg condition and is given by

$$W = -X_0 \sin 2\theta/(|\cos\theta_1 \cos\theta_2|^{1/2} k_{0r}\overline{\chi}_h). \quad (14)$$

The distance from the exact Bragg condition in the reciprocal-lattice space is X_0, the definition of which is given in equation (9) of FK. It is noted that W does not diverge if $\overline{\chi}_h \neq 0$, *i.e.* one of χ_{hi} and χ_{hr} can be zero. The parameter L is given by

$$|L^{1/2}|^2 = (A^2 + B^2)^{1/2}, \quad (15)$$

$$\text{Re } L^{1/2} = (A + |L^{1/2}|^2)^{1/2}/2^{1/2} \quad (16)$$

and

$$\text{Im } L^{1/2} = \pm(-A + |L^{1/2}|^2)^{1/2}/2^{1/2}. \quad (17)$$

In (17), the positive sign is chosen for $g'W - p\cos\delta > 0$ and the negative sign for $g'W - p\cos\delta < 0$. Here, A and B are given by

$$A = W^2 + 1 - g'^2 - b^2 \quad (18)$$

and

$$B = 2(g'W + p\cos\delta). \quad (19)$$

In the following, we treat only the σ-polarization mode. For the π-polarization mode, we obtain similar formulas by multiplying the polarization factor $|\cos 2\theta|$ by χ_{hr} and χ_{hi}. In addition, we assume that a crystal has a center of symmetry and δ is either 0 or π. Then, $\overline{\chi}_h$ in (3) is equal to the absolute value of $|\chi_h|$.

3. Rocking curves

We calculated rocking curves as functions of W in the symmetric Laue case where $\beta = \pi/2$ and therefore $g' = 0$. Fig. 1 shows rocking curves P_h/P_0 for $k = 0$ ($\chi_{hr} = 0$), $k = 1$ ($|\chi_{hr}| = |\chi_{hi}|$) and $k = \infty$ ($\chi_{hi} = 0$) when $sH = \pi$, $g_0 = -1$ and $\delta = 0$. The rocking curves of the diffracted beam are symmetric with respect to $W = 0$, regardless of the value of k.

In the case where $k = \infty$, the rocking curve shows the well known form of conventional dynamical theory. P_h/P_0 becomes zero at $W = 0$ because $sH = \pi$. In the case where $k = 1$, P_h/P_0 is about 0.25 at $W = 0$, owing to the abnormal transmission effect. In the case where $k = 0$, P_h/P_0 is about 0.25 at $W = 0$, which is the result of a new type of abnormal transmission effect pointed out by FK. The *Pendellösung* fringes are observed in all the curves. When k decreases from positive infinity to zero, the amplitude of the *Pendellösung* fringes gradually decreases. However, even for $k = 0$, the fringes are observed.

Fig. 2 shows the rocking curves of the transmitted beam P_d/P_0 for $k = 0$, 0.5, 1.0, 5.0 and ∞. The rocking curves are symmetric with respect to $W = 0$ for $k = 0$ and ∞ but not symmetric for other values of k. The asymmetry is largest when $k = 1$. When k is increased from 0.5 to 5.0, the maximum peak of each curve moves to the lower-W side from 0 to -1 and the minimum point moves similarly from 2 to 1. When $k = 0$, the abnormal transmission around $W = 0$ becomes conspicuous. In all the curves in Fig. 2, the *Pendellösung* fringes are observed. The amplitude of the fringes decreases when k is decreased, which is a similar variation to that observed in Fig. 1.

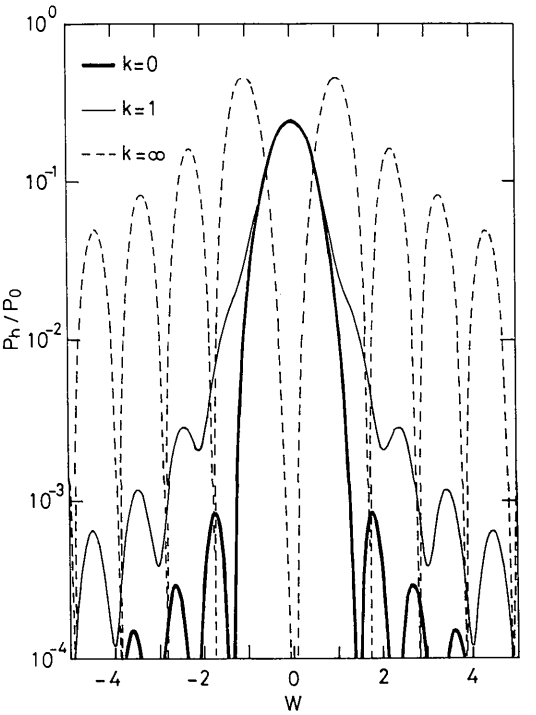

Fig. 1. The rocking curves of the diffracted beam as functions of W for $k = 0$ (thick solid line), $k = 1$ (thin solid line) and $k = \infty$ (dashed line). $sH = \pi$, $g_0 = -1$ and $\delta = 0$.

3.1. *Nontransparent effect*

In Fig. 3, the rocking curves of the transmitted beam P_d/P_0 for $k = 1$ are shown by the solid lines and values of $\exp(-\mu H')$ due to the mean absorption are shown by dashed lines for the three sH values. In the negative region of W, the P_d/P_0 are larger than $\exp(-\mu H')$; the abnormal transmission effect is observed. In the positive region of W, the P_d/P_0 are smaller than $\exp(-\mu H')$; the abnormal absorption effect is observed. A sharp decrease in P_d/P_0 is observed in each curve in Fig. 3, when neither χ_{hr} nor χ_{hi} is zero. The minimum intensity is much smaller than that expected as the abnormal absorption effect. We refer to this as a nontransparent effect. It occurs for $sH = 1.80$, 3.49 and 4.70 when $k = 1$. We label the minimum intensities appearing with increasing sH successively as the first and second nontransparent minima and so on.

The nontransparent effect is obtained for a particular combination of k, W and sH. Fig. 4(*a*) shows the plots of k *versus* sH when the first to the fourth nontransparent minima are obtained. Each dot represents a point at which a nontransparent minimum is observed. Fig. 4(*b*) shows similar plots between k and W.

The nontransparent effect is interpreted as follows. In the two-beam approximation of dynamical theory, two branches of the beams are excited in a crystal. If we denote the amplitudes of the transmitted beams for these two branches $D_0^{(1)}$ and $D_0^{(2)}$, respectively, and the normal components of the wave vectors $k_{0z}^{(1)}$ and $k_{0z}^{(2)}$, then the transmitted beam D_0 is expressed by

$$\begin{aligned}|D_0| &= |D_0^{(1)} \exp(-2\pi i k_{0z}^{(1)} z) + D_0^{(2)} \exp(-2\pi i k_{0z}^{(2)} z)| \\ &= |\exp(-2\pi i k_{0r} z \cos\theta)| \\ &\quad \times |\{(W + L^{1/2}) \exp[sz(g - \mathrm{Im}\, L^{1/2})] \\ &\quad \times \exp(isz\, \mathrm{Re}\, L^{1/2}) \\ &\quad - (W - L^{1/2}) \exp[sz(g + \mathrm{Im}\, L^{1/2})] \\ &\quad \times \exp(-isz\, \mathrm{Re}\, L^{1/2})\}/(2L^{1/2})| \\ &= |\exp(-2\pi i k_{0r} z \cos\theta)|\, |D_{0r} + iD_{0i}|. \end{aligned} \tag{20}$$

Here, D_{0r} and D_{0i} are the real and imaginary parts, respectively, of the last equation and z is the depth from the surface. Since the first term of the right-hand side of the last equation is 1, the nontransparent effect should be related to the second part. We calculate D_{0r}, D_{0i} and $|D_0|$ as functions of W for $sH = 1.5$, 1.67 and 1.84 when $g_0 = -1$ and $k = 2$. The results are shown in Fig. 5. The solid lines are D_{0r}, the dashed lines are D_{0i} and the dotted lines are $|D_0|$. For $sH = 1.5$, both D_{0r} and D_{0i} are positive at

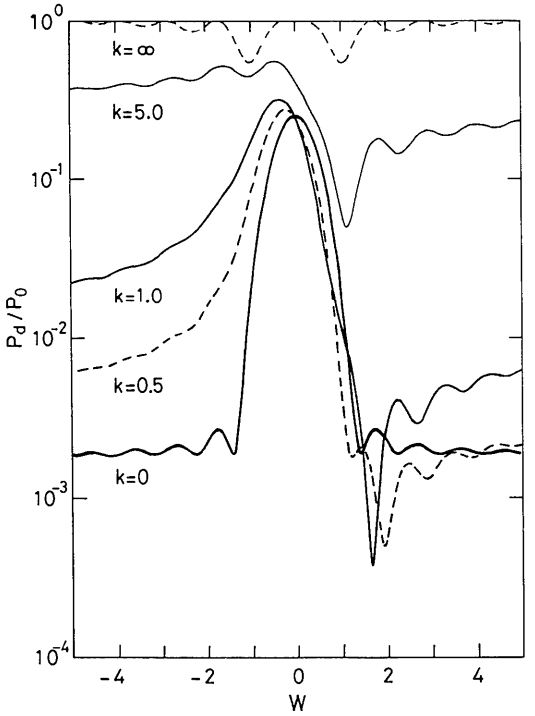

Fig. 2. The rocking curves of the transmitted beam for $k = 0$ (thick solid line), $k = 0.5$ (dashed line), $k = 1$ (solid line), $k = 5$ (thin solid line) and $k = \infty$ (thin dashed line). $sH = \pi$, $g_0 = -1$ and $\delta = 0$.

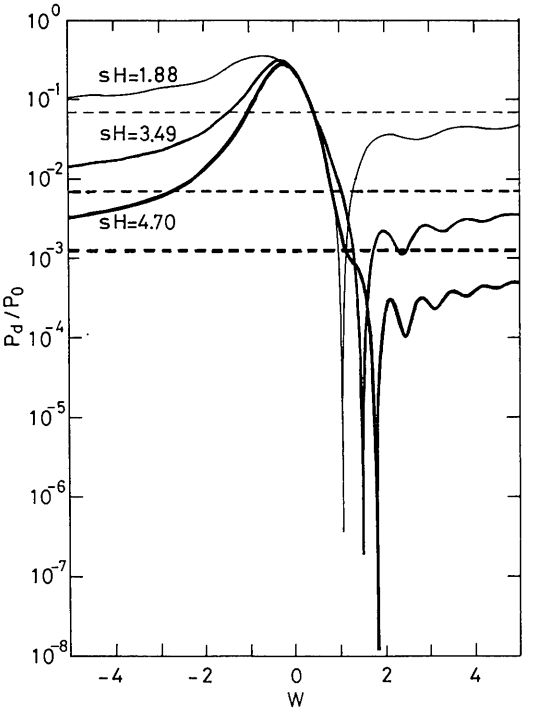

Fig. 3. The rocking curves of the transmitted beam for $sH = 4.70$ (thick solid line), $sH = 3.49$ (solid line) and $sH = 1.88$ (thin solid line). $k = 1$, $g_0 = -1$ and $\delta = 0$. The three dashed lines represent $\exp(-\mu H')$ for the above three values of sH.

the intersection A of the curves of D_{0r} and D_{0i}. For $sH = 1.84$, they are negative at the intersection. For the intermediate value $sH = 1.67$, they are zero at the intersection. The transmitted intensity should be zero when both D_{0r} and D_{0i} are zero. This corresponds to the first nontransparent minimum. For larger W, D_{0r} and D_{0i} curves intersect at the point B in Fig. 5 where neither D_{0r} nor D_{0i} is zero. When sH is further increased, both D_{0r} and D_{0i} become zero at another point, which corresponds to the second nontransparent minimum.

It is noted that the diffracted beam does not show any corresponding enhancement or reduction in intensity when the nontransparent effect is observed in the transmitted beam.

3.2 *Asymmetric reflection*

Kishino, Noda & Kohra (1972) theoretically showed that the abnormal transmission intensity in the asymmetric reflection case is larger than that in the symmetric case. By using Cr $K\alpha$ X-radiation, they measured the rocking curves of the diffracted and the transmitted beams from silicon in the asymmetric reflection case and confirmed the enhancement of the intensity. Their theoretical treatment is complicated and not analytical. In contrast, the present treatment is simple and provides an easy way to understand the phenomenon.

To examine the effect pointed out by Kishino *et al.* (1972), we calculate rocking curves of P_h/P_0 and P_d/P_0 in the asymmetric reflection case for $k = 0$ and 1. We define the asymmetric factor as

$$a = \cos\theta_1/|\cos\theta_2|. \tag{21}$$

In the symmetric case, $a = 1$.

In the case where $k = 0$, the calculated rocking curves of P_h/P_0 and P_d/P_0 are shown in Fig. 6 for $a = 0.4$, 1.0, 2.0 and 10.0. The rocking curves of both transmitted and diffracted beams are symmetric with respect to $W = 0$. The peak intensity of the diffracted beam P_h/P_0 is a maximum of 0.25 for $a = 1$. The peak intensity of the transmitted beam, on the other hand, becomes large with increasing a; it is 0.85 at $W = 0$ when $a = 10.0$, showing conspicuous abnormal transmission.

In the case where $k = 1$, the calculated rocking curves of P_h/P_0 and P_d/P_0 are shown in Fig. 7. The rocking curves of both P_h/P_0 and P_d/P_0 are asymmetric with respect to their peaks, except for $a = 1$ of

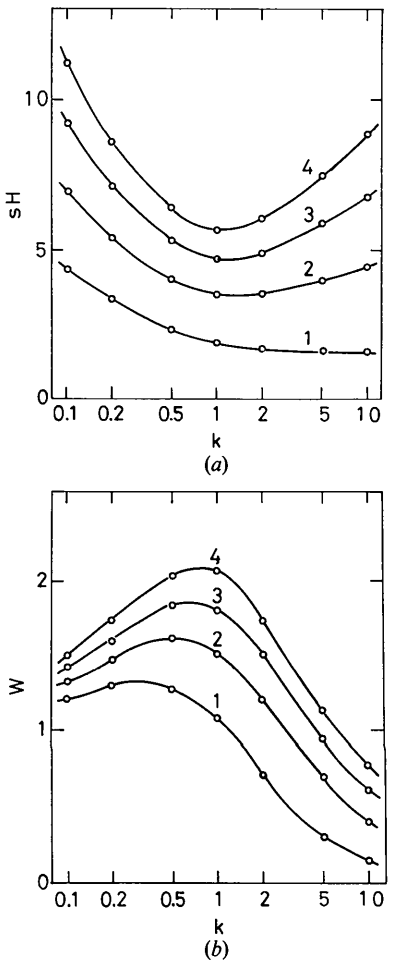

Fig. 4. The conditions in which the nontransparent effect occurs. (*a*) The relation between k and sH. (*b*) The relation between k and W. The circles show the calculated values; the lines are just given as a guide for the eye.

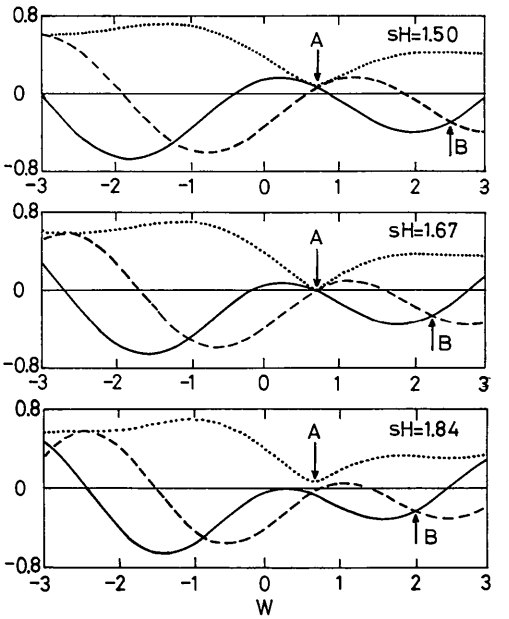

Fig. 5. The amplitudes of the transmitted beam D_{0r} (solid lines), D_{0i} (dashed lines) and $|D_0|$ (dotted lines) for $sH = 1.50$ (upper panel), $sH = 1.67$ (middle panel) and $sH = 1.84$ (lower panel); $k = 2$, $g_0 = -1$ and $\delta = 0$.

P_h/P_0. The maximum peak intensity of P_h/P_0 is 0.25 for $a = 1$, just the same as in the case of $k = 0$ in Fig. 6. The peak intensity of the transmitted beam is similar to that for $k = 0$; the peak becomes larger with increasing a. The peaks of both the diffracted and the transmitted beams shift to the smaller value of W with increasing a.

The abnormal intensity enhancement is the same effect as pointed out by Kishino *et al.* (1972) when neither the real nor the imaginary part of the polarizability is zero. We have also shown that the abnormal intensity enhancement of the transmitted beam is observed even when the real part of the X-ray polarizability is zero (in Fig. 6).

4. Integrated reflecting power

According to FK, the angle-dispersive reflecting power R_h in the Laue case is given by

$$R_h = [(\cos\theta_2/\cos\theta_1)^{1/2}/\sin 2\theta]\overline{\chi}_h \int (P_h/P_0)\,\mathrm{d}W. \quad (22)$$

It is noted that the prefactor is $\overline{\chi}_h$ instead of $|\chi_{hr}|$. In the conventional formulas (Zachariasen, 1945; Hirsch & Ramachandran, 1950; Batterman & Cole, 1964; Miyake, 1969), $|\chi_{hr}|$ is used and the integrated reflecting power is zero if $|\chi_{hr}|$ is zero even when $|\chi_{hi}|$ is not zero. In a study of *Pendellösung* fringes using spherical wave theory, Kato (1968) pointed out that the imaginary part of the structure factor should come in the prefactor of the integrated reflection intensity. Saka & Kato (1986) used $|F_h|$ as the prefactor of the integrated reflecting power and determined the crystal structure factor F_h of silicon precisely. It is obvious from Fig. 1 that the diffracted intensity P_h/P_0 is not zero and the integrated reflecting power is not zero when $k = 0$, *i.e.* $\chi_{hr} = 0$.

In Fig. 8, $R_h^w = \int (P_h/P_0)\,\mathrm{d}W$ in the Laue case is shown as a function of sH for various k. The integral R_h^w is small for small k; R_h^w for $k = 0$ is one order of magnitude smaller than that for $k = \infty$, when sH is larger than 3. The *Pendellösung* fringes are clearly seen as a function of sH for k larger than 1.

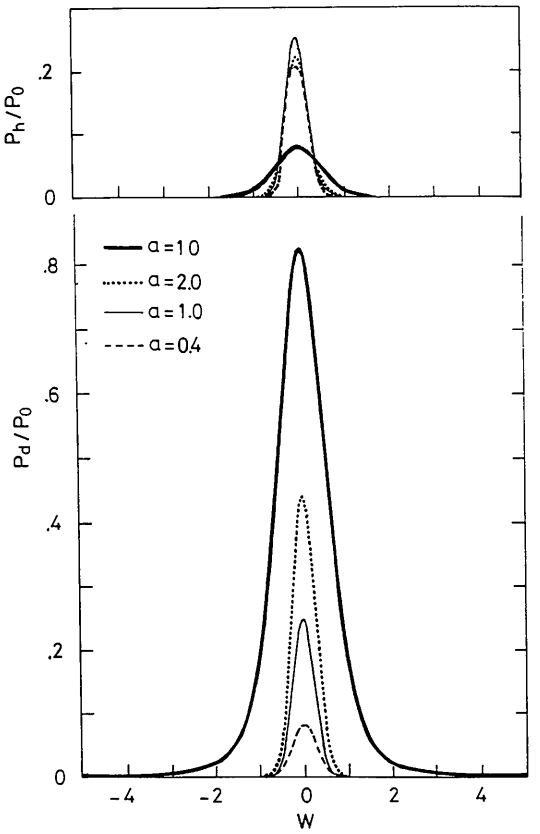

Fig. 6. The rocking curves of the diffracted beam (upper panel) and the transmitted beam (lower panel) for the asymmetric factor $a = 10.0$ (thick solid lines), $a = 2.0$ (dotted lines), $a = 1.0$ (thin solid lines) and $a = 0.4$ (dashed lines) in the case where $k = 0$, $g_0 = -1$, $\delta = 0$ and $sH = 10$.

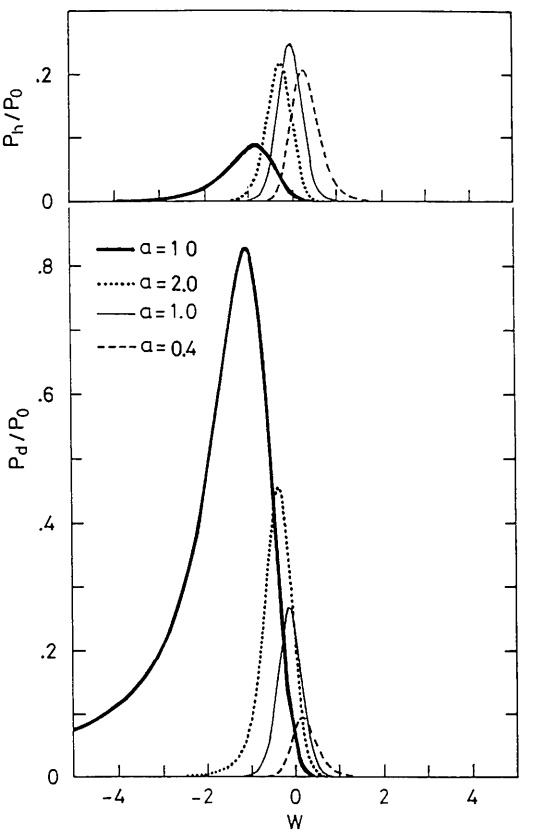

Fig. 7. The rocking curves of the diffracted beam (upper panel) and the transmitted beam (lower panel) for the asymmetric factor $a = 10.0$ (thick solid lines), $a = 2.0$ (dotted lines), $a = 1.0$ (thin solid lines) and $a = 0.4$ (dashed lines) in the case where $k = 1$, $g_0 = -1$, $\delta = 0$ and $sH = 10$.

5. X-ray polarizability apparent in the *Pendellösung* fringe

In the rocking curves shown in Figs. 1 and 2, the distance ΔW between two adjacent peaks of *Pendellösung* fringes can be obtained. From (8) or (9), we have the relation

$$sH\Delta W = \pi. \tag{23}$$

By inserting this equation into (11) and approximately k_{0r} by K_0 (the wave number in vacuum), we obtain

$$\overline{\chi}_h = |\cos\theta_1 \cos\theta_2|/(K_0 H \Delta W). \tag{24}$$

If we determine all the values of the right-hand side of (24) in the measurement of the *Pendellösung* fringes (Teworte & Bonse, 1984), we can determine $\overline{\chi}_h$. So far, $|\chi_{hr}|$ instead of $\overline{\chi}_h$ was supposed to be determined from the measurement of *Pendellösung* fringes, which is incorrect as shown above. When the ratio $|\chi_{hr}|/|\chi_{hi}| > 10$, we can determine $|\chi_{hr}|$ with an accuracy better than 1%. However, to determine $|\chi_{hr}|$ near the *K*-absorption edge, we must take the effect of $|\chi_{hi}|$ into account.

Similarly, $\overline{\chi}_h$ instead of $|\chi_{hr}|$ is to be obtained from the measurement of *Pendellösung* fringes as a function of sH in the integrated reflecting powers shown in Fig. 8. The *Pendellösung* fringe is obtained only when $|\chi_{hr}|$ is larger than $|\chi_{hi}|$ ($k > 1$). To determine $|\chi_{hr}|$ by measuring *Pendellösung* fringes, we have first to determine $|\chi_{hi}|$ and then to subtract the $|\chi_{hi}|$ from the measured $\overline{\chi}_h$.

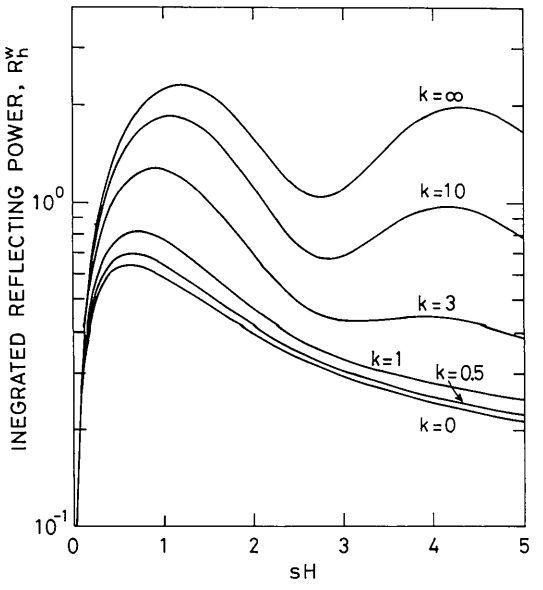

Fig. 8. R_h^w of the diffracted beam as a function of sH for several values of k.

6. Summary

We have studied dynamical diffraction in the Laue case by fully taking account of the Borrman absorption in both the symmetric and asymmetric cases. In the symmetric reflection case, all the rocking curves of the diffracted beam are symmetric with respect to $W = 0$. The rocking curves of the transmitted beams are symmetric only for $k = 0$ and ∞. They are asymmetric for other values of k and the asymmetry is largest for $k = 1$.

We have found a nontransparent effect: the transmitted beam intensity is zero for a certain combination of k, W and sH, except for $k = 0$ and $k = \infty$. We have discussed the relations between k and sH and between k and W that produce the effect.

The period of the *Pendellösung* fringes is a function of $\overline{\chi}_h$ rather than $|\chi_{hr}|$. To determine $|\chi_{hr}|$ from this period, we must subtract the contribution of $|\chi_{hi}|$, which is especially important near the *K*-absorption edge. In the determination of the structure factor of silicon from the *Pendellösung* finges in the integrated reflecting power (Saka & Kato, 1986), the relative error was estimated to be in the range 5×10^{-6} to 1×10^{-5}. The contribution of $|\chi_{hi}|$ is in the range 10^{-5} to 10^{-4} and is quite comparable to the error. For the same reason, the contribution of $|\chi_{hi}|$ must be subtracted in the determination of structure factors by the use of white X-ray *Pendellösung* fringes (Takama, Iwasaki & Sato, 1980) and by the use of X-ray resonant scattering *Pendellösung* fringes (Fukamachi, Yoshizawa, Ehara, Kawamura & Nakajima, 1990).

The authors thank Dr M. Yoshizawa, Mr K. Ehara, Professor T. Nakajima and Professor Z. Zhao for their help during the course of this study.

References

BATTERMAN, W. & COLE, H. (1964). *Rev. Mod. Phys.* **36**, 681–717.

FUKAMACHI, T. & KAWAMURA, T. (1993). *Acta Cryst.* A**49**, 384–388.

FUKAMACHI, T., NEGISHI, R., YOSHIZAWA, M., EHARA, K., NAKAJIMA, T., KAWAMURA, T. & ZHAO, Z. (1993). *Acta Cryst.* A**49**, 573–575.

FUKAMACHI, T., YOSHIZAWA, M., EHARA, K., KAWAMURA, T. & NAKAJIMA, T. (1990). *Acta Cryst.* A**46**, 945–948.

HIRSCH, P. B. & RAMACHANDRAN, G. N. (1950). *Acta Cryst.* **3**, 187–194.

KATO, N. (1968). *J. Appl. Phys.* **39**, 2225–2230, 2231–2237.

KATO, N. (1992). *Acta Cryst.* A**48**, 829–833.

KISHINO, S., NODA, A. & KOHRA, K. (1972). *J. Phys. Soc. Jpn*, **33**, 158–166.

MIYAKE, S. (1969). *X-ray Diffraction*. Tokyo: Asakura. (In Japanese.)

SAKA, T. & KATO, N. (1986). *Acta Cryst.* A**42**, 469–478.

TAKAMA, T., IWASAKI, M. & SATO, S. (1980). *Acta Cryst.* A**36**, 1025–1030.

TEWORTE, R. & BONSE, U. (1984). *Phys. Rev. B*, **29**, 2102–2108.

ZACHARIASEN, W. H. (1945). *Theory of X-ray Diffraction in Crystals*. New York: Dover.